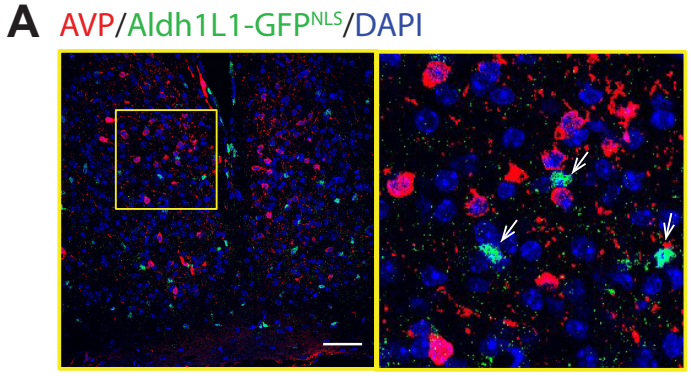

Figure S1. Aldh1L1-GFP^{NLS} does not label SCN neurons. Related to Figure 1.
(A) Astrocyte nuclei in the SCN were labeled (green) by Cre-mediated recombination of Aldh1L1-Cre/+;LSL-GFP^{NLS}/+ mice and then coronal brain sections were immunostained for AVP (red). The locations of the magnified images are indicated by yellow squares in the low-power images. Arrowheads illustrate that none of the Aldh1L1-positive cells labeled for AVP. Scale bar = 75 μm.

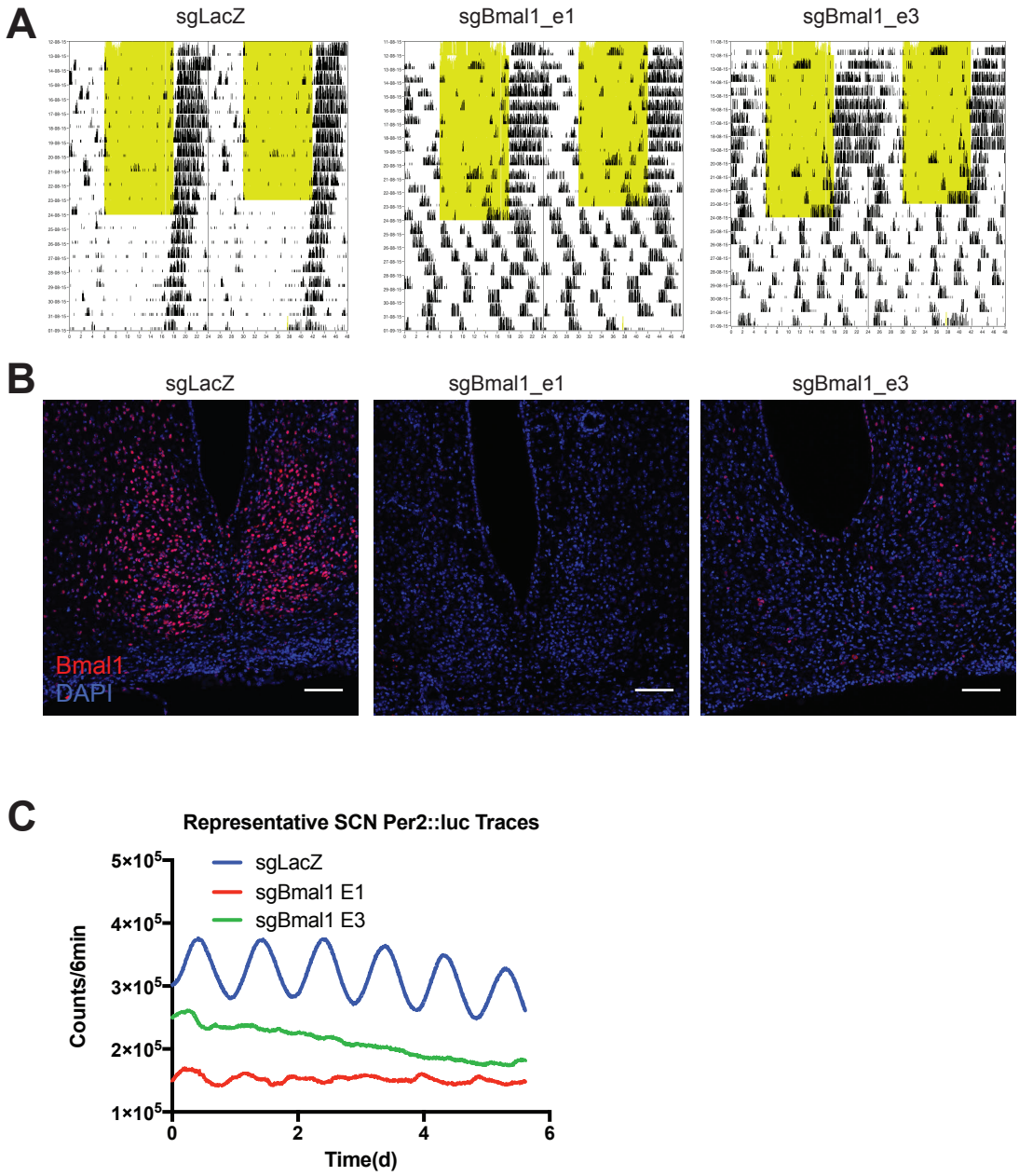

Figure S2. Loss of Bmal1 from all SCN cells phenocopies the global Bmal1 knockout. Related to Figure 3. (A) Representative actograms of LSL-Cas9/+; PER2::luc/+ animals which were injected with AAV carrying pCBh-Cre and either sgRNA against LacZ or Bmal1 (exon 1 or exon3) to the SCN. (B) BMAL1 staining (red) in the SCN of the animals shown in (A). (C) Representative PER2::luc traces from SCN slices which were infected with AAV carrying pCBh-Cre and either sgRNA against LacZ or Bmal1 (exon 1 [E1] or exon3[E3]). Note the arrhythmic PER2 expression in the two SCN where BMAL1-deletion was targeted to all cells and the circadian rhythm in the control.

Table S1: Summary statistics on AAV2/10-Bmal1ext-DIO-luc experiments. Related to Figure 2.

Genotype	Virus Added	Period	Amplitude ****	Goodness of Fit ***	Mean Bioluminescence (Counts/10min)*
Aldh1L1-Cre/+ (n = 6 mice)	AAV2/10-Bmal1ext-DIO-luc	23.6 ± 0.2 h	0.014 ± 0.002*	0.97 ± 0.007***	1,645,662 ± 578,301*
VIP-IRES-Cre (n = 4 mice)	AAV2/10-Bmal1ext-DIO-luc	23.1 ± 0.7 h	0.014 ± 0.003*	0.93 ± 0.03**	211,203 ± 13,778
WT (n = 2 mice)	AAV2/10-Bmal1ext-DIO-luc + AAV2/8-pCBh-Cre (1:1)	22.6 ± 0.1 h	0.033± 0.004****	0.98 ± 0.003**	178,785 ± 6,359
WT (n = 7 mice)	AAV2/10-Bmal1ext-DIO-luc	N.A.	0.006 ± 0.002	0.60 ± 0.07	92,647 ± 11,855

Statistics: One-way ANOVA with Bonferroni's multiple comparison test compared to no Cre control (underlined). *: $p< 0.05$; **: $p<0.01$; ***: $p< 0.001$; ****: $p<0.0001$.

Table S2. Detailed descriptions of the genetic manipulations in each figure. Related to all figures.

Glossary
Cre: Cre recombinase
Cas9: CRISPR-associated protein 9
DIO: double-floxed inverted orientation. Activated by Cre.
GFP: Green fluorescence protein
LSL: loxP-STOP-loxP. Activated by Cre
Luc: firefly luciferase
NLS: nuclear-localization signal
Rosa26: A mouse genomic locus commonly used for constitutive, ubiquitous expression.
sgBmal1_E1: sgRNA targeting exon 1 of *Bmal1*
sgBmal1_E3: sgRNA targeting exon 3 of *Bmal1*

All injections targeted the bilateral SCN.

Treatment	Full genotype	Description of genotype	Virus Injected	Description of Virus
Fig. 1 and S1				
Aldh1L1-GFP^{NLS}	Aldh1L1-Cre/+; LSL-GFP^{NLS}/+	Rosa26 knockin of LSL-GFP^{NLS} driven by ubiquitous promoter. Expression of nuclear-localized GFP was activated by Cre recombinase in Aldh1L1 (+) cells.	None.	None.
Figure 2 and Table S2				
Aldh1L1-$Bmal1^{luc}$	Aldh1L1-Cre/+	Cre recombinase was expressed in Aldh1L1 (+) cells.	AAV2/10-Bmal1ext-DIO-luc	$Bmal1^{luc}$ was activated only in Aldh1L1 (+) cells.
VIP-$Bmal1^{luc}$	VIP-IRES-Cre	Cre recombinase was expressed in vasoactive intestinal polypeptide (+) neurons.	AAV2/10-Bmal1ext-DIO-luc	$Bmal1^{luc}$ was activated only in VIP (+) neurons.
Positive Control	WT (No Cre)	WT mice.	AAV2/10-Bmal1ext-DIO-luc +	$Bmal1^{luc}$ was activated ubiquitously.

			AAV8-pCBh-Cre	
Negative Control	WT (No Cre)	WT mice.	AAV2/10-Bmal1ext-DIO-luc	Negative control to determine background bioluminescence.
Fig. 3				
Controls	LSL-Cas9-GFP/+; PER2::luc/+	Rosa26 knockin of LSL-Cas9-GFP driven by a ubiquitous promoter. Since Cre was absent, neither Cas9 nor GFP were expressed. PER2::luc was expressed in all cells.	AAV2/8-U6-sgBmal1-pCBh-mCherry^{NLS} (E1 or E3)	Ubiquitous expression of mCherry-NLS to report virus spread. In the presence of Cas9, a cut at the desired locus within the *Bmal1* gene was made. Non-homologous end joining (NHEJ) of DNA led to a frame shift and premature stop codon in the Bmal1 gene in most Cas9-expressing cells.
Aldh1L1-Bmal1-/-	Aldh1L1/+; LSL-Cas9-GFP/+; PER2::luc/+	Rosa26 knockin of LSL-Cas9-GFP driven by ubiquitous promoter. Cas9 and GFP were expressed in Aldh1L1(+) cells only. Global expression of PER2::luc.	AAV2/8-U6-sgBmal1-pCBh-mCherry^{NLS} (E1 or E3)	
Fig. S2				
sgLacZ	LSL-Cas9-GFP/+; PER2::luc/+	Rosa26 knockin of LSL-Cas9-GFP driven by ubiquitous promoter. Cas9 and GFP were expressed only in the presence of Cre recombinase. Global expression of PER2::luc.	AAV2/8-pCBh-Cre + AAV2/8-U6-sgLacZ-pCBh-mCherry^{NLS}	Ubiquitous expression of mCherry-NLS and Cre. Since lacZ is absence in the mammalian genome, sgLacZ is a control vector designed to test the specificity of sgRNA sequence.
sgBmal1 (E1 and E3)	LSL-Cas9-GFP/+; PER2::luc/+		AAV2/8-pCBh-Cre + AAV2/8-U6-sgBmal1-pCBh-mCherry^{NLS}	Ubiquitous expression of mCherry-NLS and Cre. In the presence of Cas9, a cut at a desired locus within

			(E1 or E3)	the Bmal1 gene was made and non-homologous end joining (NHEJ) of DNA leads to frame shift and premature stop codon in most Cas9-expressing cells.
Data not shown (related to fig. 3)				
AAV8-GFAP-GFP	Bmal1$^{f/f}$; PER2::luc/PER2::luc	Bmal1 conditional knockout in GFAP(+) cells. Global expression of PER2::luc.	AAV8-GFAP-GFP	GFP expression was driven by GFAP promoter.
AAV8-GFAP-Cre	Bmal1$^{f/f}$; PER2::luc/PER2::luc	Bmal1 conditional knockout. Global expression of PER2::luc.	AAV8-GFAP-Cre-GFP	Cre and GFP expression were driven by GFAP promoter.
Fig. 4a-d				
CK1ε$^{tau/+}$	CK1ε$^{tau/+}$; PER2::luc/+	Heterozygous *tau* mutation in casein kinase 1 epsilon gene led to short period (~22h) phenotype. Global expression of PER2::luc.	None.	None.
Aldh1L1-CK1ε$^{tau/+}$	Aldh1L1-Cre/+; CK1ε$^{tau/+}$; PER2::luc/+	Heterozygous *tau* mutation in casein kinase 1 epsilon gene led to short period (~22h) phenotype. The mutation was deleted in Aldh1L1(+) cells throughout the mouse, resulting in reversal of phenotype in those cells only. Global expression of PER2::luc.	None.	None.
Fig. 4e-j				
AAV8-	CK1ε$^{tau/+}$;	Heterozygous *tau* mutation in	AAV8-GFAP-GFP	GFP expression was driven

GFAP-GFP	PER2::luc/+	casein kinase 1 epsilon gene led to short period (~22h) phenotype. Global expression of PER2::luc.		by GFAP promoter.
AAV8-GFAP-Cre	$CK1\varepsilon^{tau/+}$; PER2::luc/+	Heterozygous *tau* mutation in casein kinase 1 epsilon gene led to short period (~22h) phenotype. The mutation was deleted in infected SCN GFAP(+) cells throughout the mouse, resulting in reversal of phenotype in those cells only. Global expression of PER2::luc.	AAV8-GFAP-Cre-GFP	Cre and GFP expression were driven by GFAP promoter.

Jackson Lab Stock Number or citation:

Aldh1L1-Cre/+	Jax: 023748
$CK1\varepsilon^{tau/tau}$	PMID: 18400165
LSL-Cas9-eGFP	Jax: 024858
$LSL\text{-}GFP^{NLS}$	Jax: 008516
PER2::luc	Jax: 006852
VIP-IRES-Cre	Jax: 010908
$Bmal1^{f/f}$	Jax: 007668

Supplemental Experimental Procedures

Immunohistochemistry.
Animals were sacrificed between ZT 2-4 by transcardial perfusion of PBS followed by 4% paraformaldehyde and their brains harvested and cryoprotected. We made 30 μm coronal brain sections using a cryostat. Immunostaining was performed as previously described. [S1] Primary antibodies used were rabbit anti-BMAL1 (NB100-2288, Novus, 1:5000), rabbit anti-GFAP (Z0334, Dako, 1:100), chicken anti-GFP (ab13970, Abcam, 1:2000), mouse anti-AVP (PS41, gift from Dr. Harold Gainer, NINDS, 1:50), and mouse anti-FOX2 (ab57154, Abcam, 1:200). Secondary antibodies used were Alexa Fluor 488-conjugated Goat anti-Chicken IgG, Cy3-conjugated Donkey anti-rabbit IgG, Alexa Fluor 594-conjugated Donkey anti-mouse IgG and Alexa Fluor 647-conjugated Donkey anti-rabbit IgG (all from Jackson Immuno Research, 1:500). Sections were mounted with ProLong® Gold Antifade Mountant with DAPI (Thermo Scientific). Images were acquired on a Nikon A1 confocal microscope as a single z-section (optical section thickness of 2.73μm). Images were taken sequentially averaging 4 images for each of the four-color channels. Observers blinded to the treatment groups counted cells within the SCN that expressed one or more of the targeted antigens using ImageJ software [S2].

Behavior recording.
Mice were maintained in the Danforth animal facility at Washington University. Adult mice were housed individually in cages equipped with running wheels and maintained in light-tight chambers illuminated with fluorescent bulbs (General Electric). Running wheel activity was recorded in 6-min bins (Clocklab, Actimetrics). Period was determined by χ^2 periodogram using Clocklab software.

Bioluminescence Recording.
Unless otherwise specified, 300-μm coronal SCN slices were prepared from adult animals. Briefly, mice were sacrificed with CO_2 and decapitated. Brains were quickly collected in chilled Hank's balanced salt solution (HBSS), pH 7.2 (Sigma), supplemented with 0.01 M HEPES (Sigma), 100 U/mL penicillin, 0.1 mg/mL streptomycin, and 4 mM $NaHCO_3$ (Invitrogen). Brain sections were obtained with a vibratome (OTS-5000; Electron Microscopy Sciences). Each SCN was dissected and cultured individually on a Millicell-CM membrane (Millipore) in a 35mm Petri dish with 1 mL of DMEM (Sigma) supplemented with 10 mM HEPES (Sigma), 2.2 mg/mL $NaHCO_3$ (Invitrogen), and 0.1 mM beetle D-luciferin (Biosynth). Petri dishes were sealed with vacuum grease and placed under photomultiplier tubes (HC135-11MOD; Hamamatsu) at 36 °C in the dark. Bioluminescence was recorded in 6-min bins (PER2::luc) or 10-min bins (AAV2/10-Bmal1ext-DIO-luc). Acquired *in vitro* bioluminescence traces were detrended by division and fitted with a damped sine function (Chronostar 1.0 [3]), and traces with a coefficient of correlation >0.80 and period between 18-30h were defined as circadian. The periods of PER2::luc and *Aldh1L1-Bmal1*^{luc} expression were determined using Chronostar software. For CCD recordings, *Aldh1L1-Bmal1*^{luc} SCN was imaged under 20x objective with 0.5x coupler using an ultrasensitive CCD camera (Andor iKon) mounted on an inverted microscope. Temperature was maintained at 35°C with a box incubator (In vivo Scientific). Static, cell-sized ROIs were drawn on the acquired movie in ImageJ and the acquired traces were processed through a custom Matlab script. Circadian traces from each movie were detrended by division and presented as a raster plot. We used Chronostar to determine period and rhythmicity from the raw traces. All ROIs that had a coefficient of correlation >0.80 and period between 18-30h were defined as circadian and the time of their second Bmal1-Luc peak was evaluated by a Rayleigh test of uniformity using the R package "circular". [S3]

Statistical Analysis.
All results were expressed as mean ± SEM. For comparisons of two groups of normally distributed data, Student's t-test was performed. One-way ANOVA with Sidak's multiple comparison test was used for data shown in Fig. 3e. GraphPad Prism 7 was used to perform statistical analysis and to generate figures.

Supplemental References

S1. An, S., Irwin, R.P., Allen, C.N., Tsai, C., and Herzog, E.D. (2011). Vasoactive intestinal polypeptide requires parallel changes in adenylate cyclase and phospholipase C to entrain circadian rhythms to a predictable phase. J Neurophysiol *105*, 2289-2296.

S2. Schneider, C.A., Rasband, W.S., and Eliceiri, K.W. (2012). NIH Image to ImageJ: 25 years of image analysis. Nat Methods *9*, 671-675.

S3. Maier, B., Wendt, S., Vanselow, J.T., Wallach, T., Reischl, S., Oehmke, S., Schlosser, A., and Kramer, A. (2009). A large-scale functional RNAi screen reveals a role for CK2 in the mammalian circadian clock. Genes Dev *23*, 708-718.